In vivo molecular target assessment of matrix metalloproteinase inhibition

CHRISTOPH BREMER, CHING-HSUAN TUNG & RALPH WEISSLEDER

Center for Molecular Imaging Research, Massachusetts General Hospital and Harvard Medical School, Charlestown, Massachusetts, USA
Correspondence should be addressed to C-H.T. or R.W.;
email: tung@helix.mgh.harvard.edu or weissleder@helix.mgh.harvard.edu

A number of different matrix metalloproteinase (MMP) inhibitors have been developed as cytostatic and anti-angiogenic agents and are currently in clinical testing. One major hurdle in assessing the efficacy of such drugs has been the inability to sense or image anti-proteinase activity directly and non-invasively *in vivo*. We show here that novel, biocompatible near-infrared fluorogenic MMP substrates can be used as activatable reporter probes to sense MMP activity in intact tumors in nude mice. Moreover, we show for the first time that the effect of MMP inhibition can be directly imaged using this approach within hours after initiation of treatment using the potent MMP inhibitor, prinomastat (AG3340). The developed probes, together with novel near-infrared fluorescence imaging technology will enable the detailed analysis of a number of proteinases critical for advancing the therapeutic use of clinical proteinase inhibitors.

Proteinases are essential for the normal functioning of mammalian cells and have key roles in many diseases. In cancer they impart defining characteristics—the ability of malignant cells to invade and metastasize to different tissue compartments. Intricate interactions between cancer and stromal cells control at least three major proteinase systems responsible for extracellular proteolysis: urokinase/plasminogen activator network[1], matrix metalloproteinases (MMPs)[2] and cysteine proteinases[3]. These proteinases enable malignant cells to breach basement membranes and subsequently invade[2]. Several MMPs are expressed in cancers at much higher levels than in normal tissue and the extent of expression has been shown to be related to tumor stage[4], invasiveness[5,6], metastasis[7] and angiogenesis[8]. MMP-2 (gelatinase) in particular, has been identified as one of the key MMPs in these processes, being capable of degrading type-IV collagen, the major component of basement membranes[9]. Based on the above observations, several companies have initiated the development of different MMP inhibitors to treat malignancies and other diseases involving pathologic angiogenesis[10–13].

The design of proteinase inhibitors has evolved over the last decade and now largely relies on structure-based designs[10], screening of combinatorial libraries or employing other combinatorial peptide approaches[14]. Through these efforts a number of broad-spectrum[15] and more 'selective' MMP inhibitors have been described and are in clinical trials[11,14], while a number of agents are in preclinical development.

Efficacy testing in animals has been largely measured as suppression of tumor growth based on tumor-volume measurements following treatment and by assessment of histological and anti-angiogenic effects of MMP inhibitors in human tumor xenografts. For example, prinomastat (AG3340) has been shown to be effective in slowing tumor growth rates, inducing tumor necrosis and in suppressing neovascularization in a variety of models when compared with control groups[11]. However, differences in tumor growth usually do not reach statistical significance in murine models until 10–20 days after initiation of treatment[11,14]. In a clinical setting, surrogate markers of treatment efficacy, including tumor regression, time to recurrence or time to progression, have been used because of the lack of more direct measures, although the limitations of such late endpoints are obvious. In clinical trials of the broad-spectrum MMP inhibitor marimastat (BB-2516), zymographic analysis of peripheral blood did not show any consistent patterns of change in MMP levels during treatment[16]. Similarly, in a Phase I study, the efficacy of BAY 12-9566 could not be discerned based on plasma levels of vascular endothelial growth factor or basic fibroblast growth factor[17]. Thus, there is a need to develop surrogate biomarkers to study effects of MMP inhibitors *in vivo*[18]. In addition to the above examples in single-agent trials, MMP inhibitors might be more effective when used in combination with chemotherapeutic agents[19]. A specific molecular target-based pharmacodynamic assessment of each therapeutic approach would therefore be highly beneficial (for estimating the relative contributions of each agent and resulting synergies). For the reasons outlined above we have explored the possibility of using a novel non-invasive technique to sense proteinase activities directly *in vivo* in intact tumor environments.

A number of different approaches to image molecular targets have been advocated, most of them relying on labeling target-specific molecules (affinity ligands) and imaging them after intravenous (i.v.) injection when a fraction of agent has bound to its target and the remainder of non-bound agent has been cleared. These approaches have been particularly useful for imaging receptors and cell-surface–expressed molecules, but not enzyme function in a living organism. Although some agents have been developed for measuring proteinase activity *in vitro* and in cell culture[20,21], these strategies of activatable agents have not been adapted to *in vivo* imaging until recently[22,23]. Based on calculations and prior chemical designs, we hypothesized that it should be feasible to synthesize substrates converted by MMPs into fluorescent products for non-

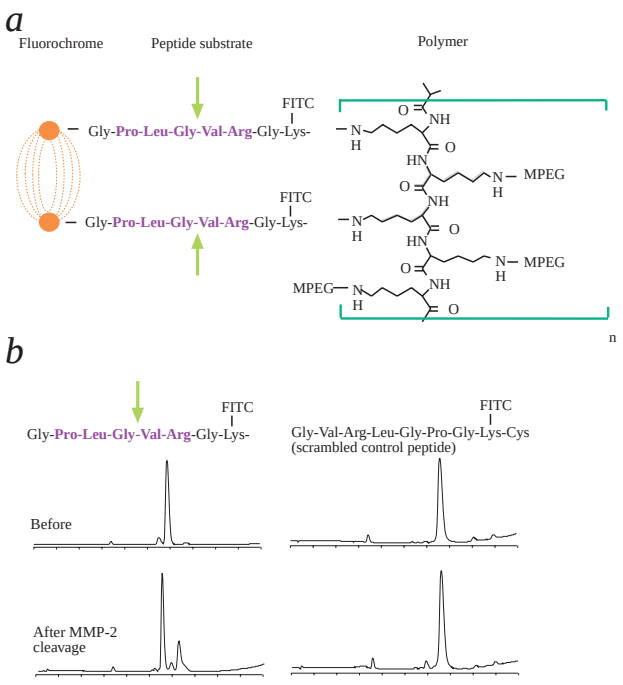

Fig. 1 MMP-2–sensitive imaging probe. ***a***, The MMP-2-sensitive imaging probes consists of 3 structural elements: The quenched NIR fluorochrome, a MMP-2 peptide substrate and a graft copolymer (methoxy-polyethylene-glycol-derivatized poly-L-lysine). ***b***, HPLC traces of utilized peptide substrates before and after MMP-2 cleavage. MMP-2-sensitive substrate (left), scrambled control peptide (right). Note that there is only cleavage of the former resulting in two degradation products. The leader Gly-Val-Arg sequence of the control peptide substrate is not recognized by MMP-2 lacking the Pro-Leu sequence.

invasive *in vivo* monitoring of enzyme activity. Recent advances in near-infrared fluorochrome design, optical imaging technology and reconstruction algorithms have facilitated imaging of fluorescent product formation. We show here for the first time that MMP activity can be imaged in live animals and that the inhibition of MMP activity can be recorded within hours after treatment by a potent MMP inhibitor, prinomastat.

Near-infrared fluorescence imaging probes

The developed imaging probes (Fig. 1) contain a preferential MMP-2 peptide substrate with quenched near-infrared fluorochromes positioned on a non-immunogenic backbone previously designed as an efficient delivery vehicle[24] (Fig. 1*a*). The rationale for this design[22] is based on high endogenous quenching of closely positioned fluorochromes, enzyme specificity imparted by conjugated peptide substrates, high loading capacity of substrates, repetitive cleavage of multiple probes by a single enzyme, and efficient tumoral accumulation through the use of stealth copolymers with a long circulation half-life[24]. Two different peptide substrates were used in this study, a MMP-2 cleavable peptide (*GPLGVRGK*(FITC)C-NH_2, substrate site is italicized[25]) and a scrambled control peptide (GVRLGPGK(FITC)C-NH_2). The ability of MMP-2 to recognize the substrates was initially confirmed by HPLC (Fig. 1*b*) showing cleavage of the former but not the latter. Although the latter control probe has a GVR leader sequence, it is too short to be recognized by MMP-2 (ref. 26). These results are also in agreement with extensive literature on MMP substrate selectivity[25].

Each assembled reporter molecule contained an average of 12 cleavable proteinase reporter groups conjugated to the amino terminus of the peptide substrate, resulting in efficient quenching of the near-infrared fluorochrome (< 90 AU at 0.3 μM concentrations of Cy 5.5). When the reporter molecules were tested *in vitro* against purified active MMP-2, fluorescence increased significantly (up to 850%; Fig 2*b*), whereas there was essentially no change in fluorescence when the control peptide was grafted onto the imaging probe (Fig. 2*a*). In order to confirm that cell-secreted MMP-2 could also activate the probe, we used conditioned medium from fibrosarcoma cells (HT1080; Fig. 3) activated with p-aminophenyl mercuric acid (APMA). As in the above studies, near-infrared fluorescence (NIRF) increased several hundred percent, whereas there was no increase using the control probe with the scrambled peptide (Fig. 2*a*). In additional studies, we also incubated the probe shown in Fig. 1*a* against a panel of MMPs: MMP-1, MMP-2, MMP-7, MMP-8 and MMP-9. The relative fluorescence increase at equimolar conditions for the different MMPs was scaled to active MMP-2 set to 100%: MMP-1, 19%; MMP-7, 12%; MMP-8, 28%; and MMP-9, 19%.

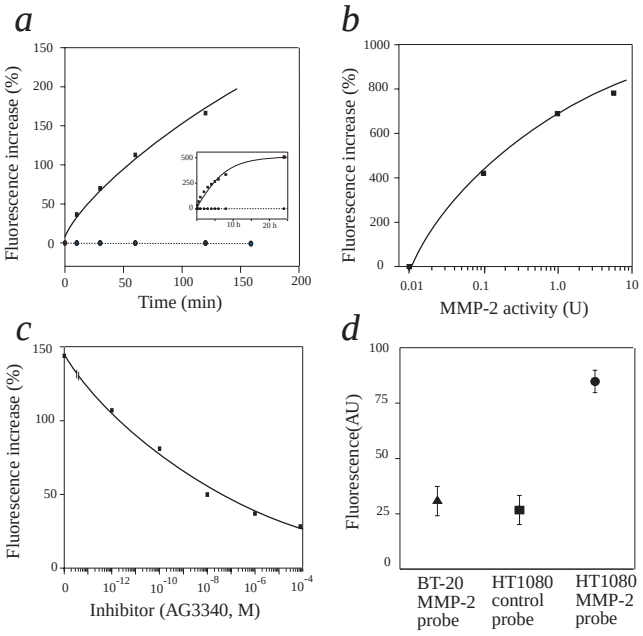

Fig. 2 Characterization of NIRF probe. ***a***, Time dependence of NIRF activation using the MMP-2-sensitive imaging probe (26.6 pmol) incubated with 6 U of MMP-2. There was no fluorescence activation when the control probe containing the scrambled peptide was used (dotted line). Likewise, there was no activation when the same experiment was conducted in the presence of 1,10-phenanthroline, a zinc chelator (data not shown). ***b***, Increase in fluorescence activation as a function of enzyme activity (26.6 pmol, 24-h incubation). ***c***, Inhibition of fluorescence activation (1 U MMP-2, 19-pmol probe) by the MMP inhibitor, prinomastat. The 50% inhibitory concentration in this assay is approximately 100 pM. ***d***, NIRFof MMP-2-positive (HT1080) and -negative (BT20) tumors grown in nude mice and probed for with either the MMP-2-specific probe or the control probe. NIRF signal in HT1080 tumors imaged with the MMP-2-specific probe was significantly higher compared with the control probe and BT20 tumors imaged with the MMP-2-specific probe ($P < 0.001$).

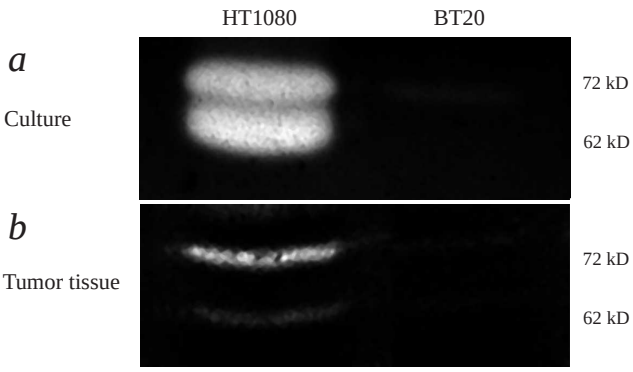

Fig. 3 MMP-2 enzyme activity in tumor models. ***a*** and ***b***, Zymography of concentrated-conditioned medium (*a*) and tumor homogenate (*b*) for HT1080 (left) and BT20 tumors (right). The 72 kD represents the pro-form and the 62 kD the activated form of MMP-2. There is considerably higher MMP-2 activity in the HT1080 when comapred to the BT20 model.

The increase in NIRF following enzyme activation occurred over at least four orders of magnitude of enzyme concentration using a constant amount of MMP-2 probe (Fig. 2*b*). Furthermore, fluorescence activation could be completely blocked by 1 mM of 1,10 phenanthroline, a broad-spectrum experimental MMP inhibitor that acts as a zinc chelator. In order to test the imaging probes against more clinically relevant inhibitors, we chose prinomastat and performed concentration-ranging experiments (Fig. 2*c*). This low-molecular-weight (M_r 423.5) synthetic MMP inhibitor potently inhibits critical MMPs, such as MMP-2, MMP-3, MMP-9, MMP-13 and MMP-14 at picomolar concentrations (K_i 30 to 300 pM (ref. 11)). Using 5 U of MMP-2 and 19 pmol of imaging probe we performed a dose-response study of prinomastat-mediated MMP inhibition (Fig. 2*c*) up to 0.1 mM of inhibitor. At the highest dose tested, the inhibitory effect was approximately 80%. We were not able to test higher concentrations of inhibitor because the compound was difficult to solubilize in aqueous media at high concentrations. Our estimated K_i was 0.1 nM (see Fig 2*c*), similar to the 0.05 ± 0.02 nM value described in the literature[11]. Complete inhibition was observed using other inhibitors (for example, 1,10 phenanthroline; data not shown).

In vivo imaging of MMP-2 expression

To test the MMP-sensitive near-infrared fluorescence probe *in vivo*, the HT1080 human fibrosarcoma tumor model was chosen because of its reported high MMP-2 production and the MMP-2 sensitivity of the developed probe; HT1080 cells also produce MMP-1, MMP-7, MMP-14, MMP-15 and MMP16 and to a lesser degree MMP-9 (ref. 27). The BT20 tumor model was chosen because of its relative lack of MMP-2 (confirmed by RT-PCR, data not shown). In subsequent experiments, zymography was used to probe for MMP-2 activity. These experiments confirmed enzymatic activity both in conditioned medium (Fig. 3*a*), as well as in tumor tissue (435 U MMP-2 per g tumor tissue; Fig. 3*b*) of HT1080 cells. In further validation studies we injected either the MMP-sensitive probe or the control probe into HT1080- or BT20-tumor bearing animals (the latter serving as another control of a low MMP-2-producing tumor[27]). Fig. 2*d* shows these *in vivo* data obtained by imaging within 1 hour after i.v. administration of the probes. The imaging results show significant differences between HT1080-bearing mice injected with the specific (85.0 ± 5.1 AU) or the control probe (27.5 ± 6.6 AU; $P < 0.001$). Furthermore, the BT20 tumors devoid of MMP yielded a significantly lower fluorescence signal compared with the HT1080 tumors when imaged with the MMP-2-sensitive probe (31.0 ± 6.6 versus 85.0 ± 5.1 AU; $P < 0.001$). This supported observations of other investigators using RT-PCR (ref. 27). The above and other results (Fig. 4) were corroborated by measurements of enzyme activities in excised tumor samples.

In vivo imaging of MMP-2 inhibition

The above results indicate the feasibility of recording native enzyme activities in tumors. We believe that this potentially represents an invaluable *in vivo* tool for elucidation of the functional contribution of specific proteinases in tumorigenesis, metastasis formation and angiogenesis. Indeed, such measurements could theoretically be performed at different resolutions, ranging from the microscopic cellular level (for example, using intravital, confocal or two-photon microscopy) to the macroscopic whole tumoral level (for example, near-infrared diffuse optical tomography, phase-array detection or reflectance imaging). The ultimate goal of the current study, however, was to extend this capability and to determine whether proteinase inhibition could be imaged *in vivo*. For these studies we implanted HT1080 tumors into nude mice and grew them to 2–3 mm in size. Animals were then treated with prinomastat (150 mg/kg, twice a day, intraperitoneally (i.p.) for 2 d) or control vehicle and were then imaged two hours after probe administration. Fig. 4 shows the MMP-2 color-encoded maps of one representative animal (Fig. 4*a*) and summarizes quantitative measurements in another 20 tumors (Fig. 4*b*). As readily visible from the raw data (Fig. 4*a*), there was significantly less

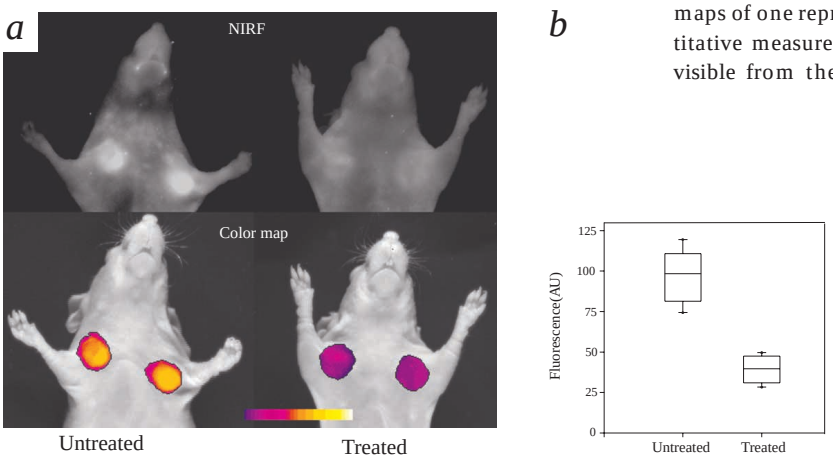

Fig. 4 *In vivo* imaging. ***a***, *In vivo* NIRF imaging of HT1080 tumor-bearing animals. The top row shows raw image acquisition obtained at 700-nm emission. Untreated (left), treated with 150 mg/kg prinomastat, twice a day, i.p. for 2 d (right). The bottom row shows color-coded tumoral maps of MMP-2 activity superimposed onto white-light images (no treatment (left), prinomastat treatment (right)). ***b***, Quantitative image analysis of all 20 tumors. Tumoral NIRF signals are shown in a box plot (bars indicate 10th and 90th percentile). The difference in imaging signal between the two groups was statistically significant ($P < 0.0001$).

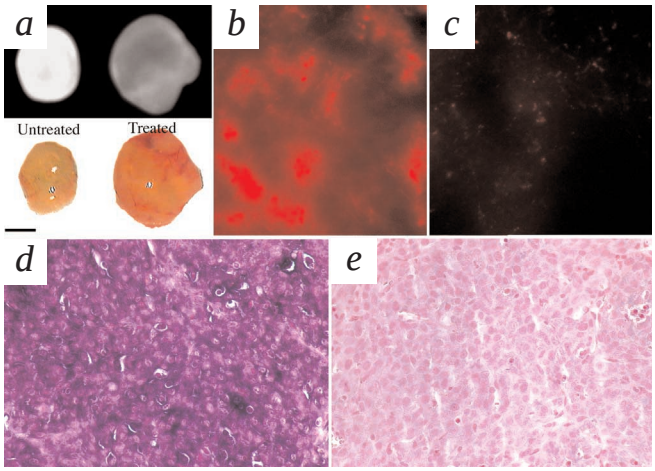

Fig. 5 Histology. ***a***, Excised HT1080 tumors from animals with and without prinomastat treatment imaged at 700 nm. Note the diminished fluorescence signal in the treated tumor. The lower row shows the corresponding light image (bar width: 1 mm). ***b*** and ***c***, NIRF microscopy of untreated (*b*) and treated (*c*) HT1080 tumors displayed at identical window and level settings (×40 objective; air-dried sections). ***d***, Immunohistochemistry of MMP-2 protein expression in HT1080 tumor section (×40 objective) counter-stained with nuclear fast red. ***e***, Same as *d* but without primary antibody for MMP-2.

MMP-2 NIRF signal in treated tumors when compared with untreated tumors. The differences in MMP-2 NIRF signal between the two groups were statistically significant (39.3 ± 3.7 AU versus 98.3 ± 5.9 AU; $P < 0.0001$). The two-day treatment reduced tumoral NIRF to nearly baseline values observed in previous control experiments (for example, compare with Fig. 2*d*). More extensive experiments are currently being conducted and initial data indicate that the technique is capable of imaging dose responses. Moreover, we have also imaged animals longitudinally before and after inhibitor treatment and shown the feasibility of imaging fluorescence activation in the same animal.

The observed *in vivo* differences in tumoral NIRF probe activation were further corroborated by processing the tumor specimen. Excised tumors from treated and non-treated animals (Fig. 5*a*) showed significant differences in NIRF when imaged at 700 nm *ex vivo* (Fig. 5*b*). Selective tumor sections were also processed for fluorescence microscopy. These data (Fig. 5*b* and *c*) further confirm a

Methods

Synthesis. The synthesized MMP-2 peptide substrate Gly-*Pro-Leu-Gly-Val-Arg-Gly*-Lys(FITC)–Cys-NH_2 (the italicized amino acids correspond to the MMP-2 substrate[25]) and the scrambled control peptide, Gly-Val-Arg-Leu-Gly-Pro-Gly-Lys(FITC)-Cys-NH_2 were confirmed by MALDI-MS. The NIRF probes were prepared according to a previously optimized method in which cathepsin D was targeted[41]. On average, each molecule contained 12 peptide reporter groups containing the terminal cyanine fluorochrome.

Characterization of NIRF probe. Initially we performed reverse-phase HPLC analysis of peptide and control substrates before and after incubation with 1 U (5 μg) of MMP-2 (Boehringer Mannheim). To test for the ability of MMP-2 to activate the entirely assembled imaging probe (Fig. 1*a*), a constant amount (26.6 pmol of imaging probe corresponding to 320 pmol Cy 5.5) was incubated with 6 U (30 μg) of activated MMP-2 (activation was achieved with 2.5 mM of p-aminophenyl mercuric acid; APMA) and fluorescence was determined over time at λ_{ex} 675 nm /λ_{em} 694 nm (Hitachi, U4500, Tokyo, Japan). To determine the range of enzyme activation, a constant amount of imaging probe (26.6 pmol) was incubated with variable amounts of activated MMP-2 and fluorescence was determined after 24 h. Inhibition experiments were performed by incubating 1 U of purified, activated MMP-2 with 19 pmol NIRF probe (220 pmol Cy 5.5) in the presence of different inhibitors, 1,10 phenanthroline (1 mM, Aldrich, Milwaukee, Wisconsin), a zinc chelator[7], or prinomastat (AG3340), a direct MMP-2 inhibitor (1×10^{-4}–10^{-12} mol; Agouron/Pfizer, San Diego, California). The latter was also used to inhibit MMP-2 for *in vivo* studies given its low K_i of 0.05 ± 0.02 nM, bioavailability and the fact that it is being tested in clinical trials[11,13]. In additional experiments we tested the MMP-sensitive probe against MMP-1, MMP-2, MMP-7, MMP-8 (Calbiochem, San Diego, California) and MMP-9 (Oncogene, Cambridge, Massachusetts). Each APMA-activated enzyme (7 pmol) was incubated for 10 min with 10 pmol of the probe at 37 °C and fluorescence was then determined. Fluorescence activation was scaled to that of APMA-activated MMP-2, which was set as 100% (4.7 AU).

Cell culture. HT1080 fibrosarcoma and BT20 mammary adenocarcinoma cells obtained from ATCC (Manassas, Virginia) were cultured in MEM medium with 2 mM L-glutamine and Earle's BSS adjusted to contain 1.5 g/l sodium bicarbonate, 0.1 mM non-essential amino acids, 1.0 mM sodium pyruvate and 10% heat-inactivated FBS.

Zymography and RT-PCR. MMP-2 enzyme activity of conditioned medium and tumor tissue was measured by zymography[42]. RT-PCR of HT1080 and BT20 cells was performed using previously published primers for MMP-2 (ref. 43).

***In vivo* studies.** 2×10^6 cells (either HT1080 or BT20) were injected subcutaneously in the mammary fat pad of athymic nude mice (nu/nu, 5–6 weeks old). Tumors were allowed to grow to 2–3 mm in size. Animals were then anesthetized and the imaging probe (167 pmol of probe per animal) was injected i.v. Imaging was typically performed 1–2 h after i.v. administration, based on a prior study in which the timing parameters had been optimized. Two different *in vivo* experiments were performed. In the first experiment, we determined the *in vivo* fluorescence activation in native HT1080 tumors probed with the MMP-2-sensitive probe ($n = 4$), HT1080 tumors probed with the control probe ($n = 4$) or the MMP-2-negative BT-20 tumors imaged with the MMP-2-sensitive probe ($n = 4$). In the second experiment, we treated HT1080 tumor-bearing animals with either prinomastat (150 mg/kg, twice a day, i.p. for 2 d, $n = 8$ tumors) or with control vehicle (twice a day i.p. for 2 d, $n = 12$ tumors). The MMP-2 probe was administered i.v. 30 min after the last of the 4 i.p. doses of prinomastat. NIRF imaging was then performed 2 h after intravenous probe administration. In other experiments, animals ($n = 4$) were imaged longitudinally before and after MMP-2 inhibitor treatment initiation.

NIRF imaging. NIRF reflectance imaging was performed using a previously described imaging system[31]. Statistical analysis of different *in vivo* groups was conducted using an ANOVA-test with Bonferroni correction for multiple comparisons. The treatment effect was tested with a two-tailed student *t*-test for paired samples. Results are presented as mean ± s.e.m.

Histology. Tumors were excised, fixed for 24 h in 10% phosphate-buffered formalin, paraffin embedded and sectioned into 7-μm slices. Immunohistochemistry was performed using a primary polyclonal goat antibody against human MMP-2 (Santa Cruz Biotechnology, Santa Cruz, California). An alkaline phosphatase-labeled rabbit anti-goat antibody was used to reveal binding of the primary antibody. Sections were counter-stained with nuclear fast red. For NIRF fluorescence microscopy tumors were snap frozen and cryosectioned into 8–10-μm slices. Air-dried sections were then viewed in phase-contrast or fluorescence mode using an inverted epifluorescence microscope (Zeiss Axiovert, Thornwood, New York).

significant difference in NIRF between the two experimental groups. MMP-2 expression in HT1080 tumors is shown by immunohistochemistry (Fig. 5*d*).

Discussion

The above results indicate that MMP (and specifically MMP-2) enzyme activity can be recorded *in vivo* using similar fluorescence activation methodology that it is used to analyze activities in *in vitro* assays[28]. In order to adapt the probe-activation paradigm for *in vivo* use, a number of fundamental design changes had to be made. First, to deliver the proteinase substrate efficiently to tumors (evading rapid renal clearance of substrate peptides), the peptide stalks were positioned onto graft copolymers previously tested in clinical trials[29]. Second, rather than using a fluorochrome and a quencher for each peptide substrate as are commonly used in *in vitro* assays, we chose a fluorochrome with overlapping excitation and emission spectrum to achieve self-quenching, ultimately yielding higher fluorescence activation upon cleavage. Finally, as light travels through tissue more efficiently in the near-infrared spectrum[30], we used near-infrared fluorochromes for readout at 700 nm, recognizing that even more red-shifted dyes might further improve the detection threshold. Moreover, it is also conceivable to use multispectral analysis with the current probe design, assaying for different enzymes simultaneously at different wavelengths.

Although the proteinase probe design and optimization represents one aspect of this research, another aspect relates to how to best detect fluorescence activation *in vivo*, both in experimental animals and ultimately in humans. For the reported experimental studies, we used a NIRF reflectance imaging system, which operates similarly to a microscope but at the macroscopic level[31]. As such, effective tissue penetration of light is limited to several millimeters. This degree of penetrance was sufficient for readout of the relatively superficial subcutaneous tumors (< 10 mm) studied in these experiments. Recently, however, alternative detection methodology has been developed. One such technique is fluorescence-mediated tomography (FMT), a method that uses advanced photon technology and mathematical modeling to produce three-dimensional (3-D) images of fluorescence activation in deep tissues. FMT uses principles of diffraction tomography that allow the quantitative assessment of NIRF probe activation in deep tissue and their 3-D localization. At appropriate wavelengths, such measurements can further calculate chromophore and fluorophore concentrations. In preliminary studies, a related technique (diffuse optical tomography) has already been used to image tricarbocyanine dye accumulation in human breast cancers[32]. The implementation of FMT systems for *in vivo* imaging can directly drive the developments of specific NIRF probes in clinically relevant applications by identifying the limits for early cancer detection and facilitating imaging of the time-course of enzymatic activation. Another detection system is based on phase-array technology relying on NIRF-induced phase-wave cancellation, capable of detecting picomolar amounts of dyes in deep tissues[30]. The extension of these technologies to detect *in vivo* fluorescence activation described here lends itself to clinical development.

We expected this technique of measuring enzyme activities to have profound impacts on a variety of clinical and experimental studies. A number of MMP-inhibitors have undergone clinical trials, such as neovastat, marimastat, BAY 12-9566 and prinomastat[12]. The approaches currently available to monitor MMP inhibition therapies rely on indirect evidence of target-based therapy, such as tumor markers, tumor size, histological changes and possibly MMP levels in blood or tumor tissue measured over a long period of time[11,16,19,33,34]. These approaches do not provide a reliable endpoint for assessing inhibition of MMP activity *in vivo*. It is expected that direct methods of molecular target assessment, as developed in this study, will benefit the myriad of MMP inhibitor studies that are under way. Indeed, the probes and technology are certainly not limited to proteinase probing in cancer, but may be used for cardiovascular[35], dermatologic[36], ophthalmic (macular degeneration[37]), infectious[38], immunologic[39], neurodegenerative[40] and other diseases. Ultimately, changing the reporter group within the NIRF probe may enable detection of other enzyme functions (and their therapeutic inhibition), for example, kinases, transferases or polymerases.

Acknowledgments

The authors would like to thank A. Bogdanov for providing the graft copolymer and U. Mahmood and A. Moore for technical assistance in imaging and animal preparation. The authors also gratefully acknowledge the assistance of S. Bredow for optimizing RT-PCR and zymography conditions. The authors would also like to thank Agouron Pharmaceuticals and Pfizer for providing prinomastat, and R. Feeley, S. Gregory and D. Shalinsky (Department of Research Pharmacology) for helpful discussions and critical review of the manuscript. This project is supported in part by NIH CA088365 and a RSNA seed grant. C.B. was supported by the Deutsche Forschungsgemeinschaft.

1. Ossowski, L., Clunie, G., Masucci, M.T. & Blasi, F. *In vivo* paracrine interaction between urokinase and its receptor: Effect on tumor cell invasion. *J. Cell Biol.* **115**, 1107–1112 (1991).
2. Chambers, A.F. & Matrisian, L.M. Changing views of the role of matrix metalloproteinases in metastasis. *J. Natl. Cancer Inst.* **89**, 1260–1270 (1997).
3. Frosch, B.A., Berquin, I., Emmert-Buck, M.R., Moin, K. & Sloane, B.F. Molecular regulation, membrane association and secretion of tumor cathepsin B. *APMIS* **107**, 28–37 (1999).
4. Stearns, M.E. & Wang, M. Type IV collagenase (M(r) 72,000) expression in human prostate: Benign and malignant tissue. *Cancer Res.* **53**, 878–883 (1993).
5. Davies, B. *et al.* Levels of matrix metalloproteases in bladder cancer correlate with tumor grade and invasion. *Cancer Res.* **53**, 5365–5369 (1993).
6. Zucker, S. *et al.* Measurement of matrix metalloproteinases and tissue inhibitors of metalloproteinases in blood and tissues. Clinical and experimental applications. *Ann. N.Y. Acad. Sci.* **878**, 212–227 (1999).
7. Moses, M.A. *et al.* Increased incidence of matrix metalloproteinases in urine of cancer patients. *Cancer Res.* **58**, 1395–1399 (1998).
8. Fang, J. *et al.* Matrix metalloproteinase-2 is required for the switch to the angiogenic phenotype in a tumor model. *Proc. Natl. Acad. Sci. U.S.A.* **97**, 3884–3889 (2000).
9. Morgunova, E. *et al.* Structure of human pro-matrix metalloproteinase-2: Activation mechanism revealed. *Science* **284**, 1667–1670 (1999).
10. Whittaker, M., Floyd, C.D., Brown, P. & Gearing, A. Design and therapeutic application of matrix metalloprotease inhibitors. *Chem. Rev.* **99**, 2735–2776 (1999).
11. Shalinsky, D.R. *et al.* Broad antitumor and antiangiogenic activities of AG3340, a potent and selective MMP inhibitor undergoing advanced oncology clinical trials. *Ann. N.Y. Acad. Sci.* **878**, 236–270 (1999).
12. Brown, P. Clinical studies with matrix metalloproteinase inhibitors. *APMIS* **107**, 174–180 (1999).
13. Nelson, A.R., Fingleton, B., Rothenberg, M.L. & Matrisian, L.M. Matrix metalloproteinases: Biologic activity and clinical implications. *J. Clin. Oncol.* **18**, 1135–1149 (2000).
14. Koivunen, E. *et al.* Tumor targeting with a selective gelatinase inhibitor. *Nature Biotechnol.* **17**, 768–774 (1999).
15. Drummond, A.H. *et al.* Preclinical and clinical studies of MMP inhibitors in cancer. *Ann. N.Y. Acad. Sci.* **878**, 228–235 (1999).
16. Wojtowicz-Praga, S. *et al.* Phase I trial of Marimastat, a novel matrix metalloproteinase inhibitor, administered orally to patients with advanced lung cancer. *J. Clin. Oncol.* **16**, 2150–2156 (1998).
17. Erlichman, C. *et al.* Phase I study of the matrix metalloproteinase inhibitor, BAY 12-9566. *Ann. Oncol.* **12**, 389–395 (2001).
18. Zucker, S. Experimental models to identify antimetastatic drugs: Are we there yet? A position paper. *Ann. N.Y. Acad. Sci.* **878**, 208–211 (1999).
19. Haq, M., Shafii, A., Zervos, E.E. & Rosemurgy, A.S. Addition of matrix metalloproteinase inhibition to conventional cytotoxic therapy reduces tumor implantation and prolongs survival in a murine model of human pancreatic cancer. *Cancer Res.* **60**, 3207–3211 (2000).
20. Van Noorden, C.J. *et al.* Ala-Pro-cresyl violet, a synthetic fluorogenic substrate for the analysis of kinetic parameters of dipeptidyl peptidase IV (CD26) in individual living rat hepatocytes. *Anal. Biochem.* **252**, 71–77 (1997).
21. Van Noorden, C.J. *et al.* Heterogeneous suppression of experimentally induced colon cancer metastasis in rat liver lobes by inhibition of extracellular cathepsin B. *Clin. Exp. Metastasis* **16**, 159–167 (1998).
22. Weissleder, R., Tung, C.H., Mahmood, U. & Bogdanov, A., Jr. *In vivo* imaging of tu-

mors with protease-activated near-infrared fluorescent probes. *Nature Biotechnol*. **17**, 375–378 (1999).
23. Tung, C.H., Mahmood, U., Bredow, S. & Weissleder, R. *In vivo* imaging of proteolytic enzyme activity using a novel molecular reporter. *Cancer Res.* **60**, 4953–4958 (2000).
24. Marecos, E., Weissleder, R. & Bogdanov, A., Jr. Antibody-mediated versus nontargeted delivery in a human small cell lung carcinoma model. *Bioconjug. Chem.* **9**, 184–191 (1998).
25. Seltzer, J.L. *et al.* Cleavage specificity of human skin type IV collagenase (gelatinase). Identification of cleavage sites in type I gelatin, with confirmation using synthetic peptides. *J. Biol. Chem.* **265**, 20409–20413 (1990).
26. Niedzwiecki, L., Teahan, J., Harrison, R.K. & Stein, R.L. Substrate specificity of the human matrix metalloproteinase stromelysin and the development of continuous fluorometric assays. *Biochemistry* **31**, 12618–12623 (1992).
27. Giambernardi, T.A. *et al.* Overview of matrix metalloproteinase expression in cultured human cells. *Matrix Biol*. **16**, 483–496 (1998).
28. Knight, C.G., Willenbrock, F. & Murphy, G. A novel coumarin-labelled peptide for sensitive continuous assays of the matrix metalloproteinases. *FEBS Lett.* **296**, 263–266 (1992).
29. Callahan, R.J., Bogdanov, A., Jr., Fischman, A.J., Brady, T.J. & Weissleder, R. Preclinical evaluation and Phase I clinical trial of a 99mTc-labeled synthetic polymer used in blood pool imaging. *Am. J. Roentgenol.* **171**, 137–143 (1998).
30. Chance, B. Near-infrared images using continuous, phase-modulated, and pulsed light with quantitation of blood and blood oxygenation. *Ann. N.Y. Acad. Sci.* **838**, 29–45 (1998).
31. Mahmood, U., Tung, C.H., Bogdanov, A., Jr. & Weissleder, R. Near-infrared optical imaging of protease activity for tumor detection. *Radiology* **213**, 866–870 (1999).
32. Ntziachristos, V., Yodh, A.G., Schnall, M. & Chance, B. Concurrent MRI and diffuse optical tomography of breast after indocyanine green enhancement. *Proc. Natl. Acad. Sci. U.S.A.* **97**, 2767–2772 (2000).
33. Lozonschi, L. *et al.* Controlling tumor angiogenesis and metastasis of C26 murine colon adenocarcinoma by a new matrix metalloproteinase inhibitor, KB-R7785, in two tumor models. *Cancer Res.* **59**, 1252–1258 (1999).
34. Maekawa, R. *et al.* Correlation of antiangiogenic and antitumor efficacy of N-biphenyl sulfonyl-phenylalanine hydroxiamic acid (BPHA), an orally-active, selective matrix metalloproteinase inhibitor. *Cancer Res.* **59**, 1231–1235 (1999).
35. Ross, R. Atherosclerosis—an inflammatory disease. *N. Engl. J. Med.* **340**, 115–126 (1999).
36. Tsukifuji, R., Tagawa, K., Hatamochi, A. & Shinkai, H. Expression of matrix metalloproteinase-1, -2 and -3 in squamous cell carcinoma and actinic keratosis. *Br. J. Cancer* **80**, 1087–1091 (1999).
37. Plantner, J.J., Jiang, C. & Smine, A. Increase in interphotoreceptor matrix gelatinase A (MMP-2) associated with age-related macular degeneration. *Exp. Eye Res.* **67**, 637–645 (1998).
38. Holskin, B.P. *et al.* A continuous fluorescence-based assay of human cytomegalovirus protease using a peptide substrate. *Anal. Biochem.* **227**, 148–155 (1995).
39. Ishiguro, N., Ito, T., Miyazaki, K. & Iwata, H. Matrix metalloproteinases, tissue inhibitors of metalloproteinases, and glycosaminoglycans in synovial fluid from patients with rheumatoid arthritis. *J. Rheumatol.* **26**, 34–40 (1999).
40. Giraudon, P., Buart, S., Bernard, A. & Belin, M.F. Cytokines secreted by glial cells infected with HTLV-I modulate the expression of matrix metalloproteinases (MMPs) and their natural inhibitor (TIMPs): Possible involvement in neurodegenerative processes. *Mol. Psychiatry* **2**, 107–110, 184 (1997).
41. Tung, C.H., Bredow, S., Mahmood, U. & Weissleder, R. Preparation of a cathepsin D sensitive near-infrared fluorescence probe for imaging. *Bioconjug. Chem.* **10**, 892–896 (1999).
42. Brown, P.D., Levy, A.T., Margulies, I.M., Liotta, L.A. & Stetler-Stevenson, W.G. Independent expression and cellular processing of Mr 72,000 type IV collagenase and interstitial collagenase in human tumorigenic cell lines. *Cancer Res.* **50**, 6184–6191 (1990).
43. Collier, I.E. *et al.* H-ras oncogene-transformed human bronchial epithelial cells (TBE-1) secrete a single metalloprotease capable of degrading basement membrane collagen. *J. Biol. Chem.* **263**, 6579–6587 (1988).

ON THE MARKET

GEL BOXES

C.B.S. Scientific offers a line of color-coded horizontal gel systems designed to help differentiate use by specific labs or for specific purposes. Available in five fluorescent colors, these Mini-Gel or Midi-Gel systems feature tapered baffles for leak-proof gel formation, UV-transparent gel beds, and safety covers with attached power leads. The horizontal mini-gel system is offered with a gel bed size of either 5.5 x 8.5 cm or 7.5 x 10 cm. Both sizes accommodate several different comb thicknesses and formats. As little as 2 µl of sample is required per sample well, says the company. Three sizes of the midi-gel system are available: 10.5 x 11 cm, 14 x 10 cm and 14 x 16 cm. They are suitable for use with a variety of polycarbonate or Teflon-coated aluminum combs.
Tel. (+1) 858-755-4959
www. cbsscientific.com

CHROMATOGRAPHY COLUMNS

Dionex introduces the ProPac WAX-10 (weak anion exchange) and SAX-10 (strong anion exchange) columns for high-resolution analysis of proteins with small differences in charge and structure. ProPac resin uses a surface-controlled polymerization technology. The packing substrate is a highly crosslinked core (which makes the packing solvent-compatible) grafted with a neutral, hydrophilic layer to eliminate hydrophobic interactions with proteins. This layer is then grafted with a polymer layer of controlled thickness that contains the anion-exchange functional group (tertiary amine for the WAX-10 and quaternary ammonium for the SAX-10). These columns are said to have a moderate capacity and are stable over a pH range of 2–10. They are suitable for characterization and quality-control assays of closely related protein variants, including acidic proteins, phosphorylated proteins, glycosylated protein variants and sialylated proteins.
Tel. (+1) 408-737-0700
www.dionex.com

ASSORTED KITS AND REAGENTS

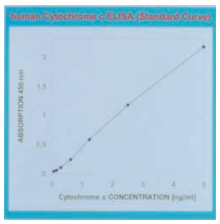

Cytochrome c ELISA

A new ELISA kit for the quantitative detection of human cytochrome c in cell culture lysates, human whole blood or serum is now offered by Bender MedSystems. This ELISA provides researchers with a new tool for detecting the activation of apoptotic programs in cells. Recent research involving serum from patients with hematological malignancies indicates that serum-cytochrome c monitoring might also serve as a clinical marker that indicates the onset of apoptosis and cell turnover *in vivo*.
Tel. (+43) 1-796-4040-0
www.bendermedsystems.com

A DNA fragmentation kit based on the terminal deoxynucleotidyl transferase-mediated dUTP nick-end labeling (TUNEL) method has been added to Clontech's ApoAlert line of apoptosis detection products. The ApoAlert DNA fragmentation assay kit is based on the direct incorporation of fluorescein-dUTP at the free 3′-hydroxyl ends of DNA fragments produced during apoptosis. Direct incorporation of the fluorescein tag is designed to save time and reduce nonspecific background. The assay can be performed on cultured cells, as well as formalin-fixed, paraffin-embedded tissue sections.
Tel. (+1) 415-424-8222
www.clontech.com

A new brochure from Alexis Biochemicals outlines almost a dozen new products for apoptosis research. Among the highlighted apoptosis detection products are antibodies and antisera to Smac/DIABLO, FLIP, BAFF, TACI and BCMA. Also featured are TRAIL receptor pathway products, including the new KillerTRAIL and monoclonal antibody to TRAIL, as well as other popular soluble TRAIL, TRAIL receptors and antibodies.
Tel. (+1) 858-658-0065
www.alexis-corp.com